Trans. Phenom. Nano Micro Scales, 6(1): 60-71, Winter and Spring 2018
DOI: 10.7508/tpnms.2018.01.006

ORIGINAL RESEARCH PAPER

Possessions of viscous dissipation on radiative MHD heat and mass transfer flow of a micropolar fluid over a porous stretching sheet with chemical reaction

Shaik. Mohammed. Ibrahim [1,*], prathi. Vijaya Kumar [1], CSK. Raju[2]

[1]Dept. of Mathematics, GITAM University, Vishakhapatnam, - 530045, India
[2]Dept. of Mathematics, VIT University, Vellore - 632014, India

Received 10 October 2016; revised 1 January 2017; accepted 11 January 2017; available online 1 January 2018

ABSTRACT: This article presents the heat and mass transfer characteristics of unsteady MHD flow of a viscous, incompressible and electrically conducting micropolar fluid in the presence of viscous dissipation and radiation over a porous stretching sheet with chemical reaction. The governing partial differential equations (PDEs) are reduced to ordinary differential equations (ODEs) by applying suitable similarity transformations which are then solved numerically using fourth order Runge-Kutta method. The results are depicted graphically for velocity, angular velocity, temperature and concentration profiles for various values of parameters such as unsteadiness parameter, magnetic parameter, porous parameter, thermal Grashof number, solutal Grashof number, Prandtl number, thermal radiation parameter, Eckert number, Schmidt number and chemical reaction parameter. To check the accuracy of our numerical code, comparison is made with the existing results. The influence of various parameters on skin friction coefficient, couple stress and rates of heat and mass transfer coefficients are presented numerically in tabular form.

KEYWORDS: *Chemical reaction; Heat and mass transfer; Micropolar fluid; Porous medium; Thermal radiation; Viscous dissipation*

INTRODUCTION

Eringen [1] introduced the theory of simple microfluids. According to this theory the simple microfluid is a fluent medium whose properties and behaviour are affected by the local motion of the fluid elements. These fluids can support body moments and stress moments and are influenced by the spin inertia. The stress tensor for these fluids is non-symmetric. This theory has presented an excellent model to examine many complex fluids some of them are liquid crystals, the flow of low concentration suspensions, blood and turbulent shear flows. Eringen [2] simplified the theory of microfluids and defined a subclass of these fluids called micropolar fluids. This theory is one of the best established theories of fluids with microstructure. Micropolar fluids represent fluids consisting of rigid randomly oriented particles suspended in a viscous medium, where the deformation of particles is ignored. The attractiveness and power of the model of micropolar fluids lie in the fact that it is both a significant and a simple generalization of the classical Navier-Stokes model. Ariman et al. [3-4], Siddheshwar and Pranesh [5, 6] have discussed the various applications of micropolar fluids.

In manufacturing processes, the boundary layer flow induced by stretching surface has various theoretical and technical applications. Some of these applications include wire drawing, paper production, glass-fiber production, liquid metal, polymer sheet synthesis, continuous stretching of plastic films and artificial fibers etc. The pioneering work in this area was carried out by Sakiadis [7]. Peddieson and McNitt [8] investigated the boundary layer flow of micropolar fluid. Various aspects of micropolar fluid flows from a stretching surface have been studied by many authors [9–15].

Magnetohydrodynamics is the branch of continuum mechanics which deals with the motion of an electrically conducting fluid in the presence of a magnetic field. Many technological problems and natural phenomena are susceptible to MHD analysis. Engineers apply MHD principle, in the design of heat exchangers, in creating novel power generating systems, pumps and flow meters, thermal protection, braking, control and re-entry, in space vehicle propulsion. MHD convection flow problems are also very important in the fields of stellar and planetary magnetospheres, aeronautics, electronics and chemical engineering. Many theoretical studies of magneto-micropolar fluids have been reported by different researchers [16-22].

The flow of micropolar fluid over a porous stretching sheet was studied by Kelson and Desseaux [23] and Kelson and Farrell [24]. Bhargava et al. [25] studied the suction effect on micropolar fluid driven by a polar stretching sheer. Micropolar fluid flow over a nonlinear stretching sheet was presented by Hayat et al. [26].

The effects of radiation on unsteady free convection flow and heat transfer problem have become more important industrially. At high operating temperature, radiation effect can be quite significant. Many processes in engineering areas occur at high temperature and knowledge of radiation

*Corresponding Author Email: *ibrahimsvu@gmail.com*
Tel.: +919866370769; Note. This manuscript was submitted on October 10, 2016; approved on January 1, 2017; published online *January 1, 2018*

Nomenclature

(u,v)	Velocity components along the x and y axes
ν	Kinematic viscosity
A	Positive constant with dimension per time
B	Constant with dimension temperature over length
B_0	Applied magnetic field
C	Concentration of the solute
C_p	Specific heat at constant pressure
C_w	Concentration of the solute at the sheet
C_∞	Concentration of the solute far from the sheet
G	Acceleration due to gravity
k	Kinematic micro-rotation viscosity
K^*	Thermal conductivity
K_p^*	Permeability of the porous medium
N	Micro-rotation component
T	Temperature of fluid
T_W	Wall temperature of the fluid
T_∞	Temperature of the fluid far away from the sheet
J	Micro-inertia density
q_r	Radiative heat flux
D_m	Molecular diffusivity
K_r	Chemical reaction parameter
D_m	Molecular diffusivity
σ^*	Stefan-Boltzman constant
K^*	Rosseland mean absorption coefficient
Gc	Solutal Grashof number
Pr	Prandtl number
B	Non-dimensional parameter
Ec	Eckert number
R	Thermal radiation parameter
Sc	Schmidt number
γ	Chemical reaction parameter
C_{fx}	Local skin friction factor
C_{sx}	Couple stress factor
Nu_x	Local Nusselt number
Sh_x	Local Sherwood number
Re_x	Reynolds number
U_w	Sheet velocity
f	Non-dimensional velocity
h	Non-dimensional angular momentum
t	Non-dimensional time
A	Unsteadiness parameter
K	Micropolar parameter
M	Magnetic field parameter
k_p	Porous parameter
Gr	Thermal Grashof number

Greek Symbols

α	Stretching rate
β	Coefficient of viscosity
ρ	Density of the fluid
σ	Electrical conductivity
γ	Spin gradient viscosity
η	Similarity variable
τ_w	Wall shear stress
Ψ	Stream function
λ_0	Non-dimensional material parameter
θ	Non-dimensional temperature
Φ	Non-dimensional concentration

Subscripts

ω	Condition at wall
∞	Condition at free stream

heat transfer becomes very important for design of reliable equipments, nuclear plants, gas turbines and various propulsion devices or aircraft, missiles, satellites and space vehicles.

Rahman and Sattar [27], Bhattacharya et al. [28] and Raptis [29] investigated thermal radiation effect on micropolar fluids. Ali and Magyari [30] have studied the characteristics of heat flow of unsteady fluid by a submerged stretching surface while its steady motion is slowed down gradually. Ishak et al. [31] presented the unsteady flow of micropolar fluid over a stretching sheet. Ibrahim et al. [32] investigated the impact of thermal radiation on MHD free convection flow of a micropolar fluid past a stretching surface embedded in a non-Darcian porous medium. Mabood et al. [33] investigation the effects of non-uniform heat source and radiation effects on magnetohydrodynamic convective flow past a stretching sheet in a micopolar fluid embedded in non-Darcian porous medium. The heat and mass transfer characteristics of micropolar fluids under different situations studied by many researchers for example Qasim and Hayat [34], ElAziz [35] and Hsiao [36]. In modern technology, considerable interest has been developed in the study of chemical reaction with combined heat and mass transfer, owing to its wide range of applications in science and technology. A good insight of this division is given by Cortell [37], Mohamed and AdoDahab [38], Pal and Biswas [39] and Mabood and Ibrahim [40].

Unsteady free convection non-Newtonian fluids have many applications in geophysics, turbo machinery and many other fields. Motivated by these applications and previous work done, we studied the effects of chemical reaction, viscous dissipation and thermal radiation on unsteady mixed convection heat and mass transfer flow of a micropolar fluid past a stretching sheet through porous media. A uniform magnetic field is applied transversely to the direction of the flow. Similarity transformations are used to convert the governing time dependent non-linear boundary layer equations into a system of non-linear ordinary differential equations that are solved numerically

by Runge–Kutta fourth order method with shooting technique.Different values of physical parameters are tabulated and discussed numerically and graphically.

MATHEMATICAL FORMULATION

We consider an unsteady two-dimensional, heat and mass transfer, free convection boundary layer flow of a viscous, incompressible, micropolar fluid past a semi-infinite permeable stretching sheet embedded in a homogeneous porous medium coinciding with the plane *y=0*, then the flow is occupied above the sheet *y>0*. A schematic representation of the physical model and coordinates system is presented in Figure 1.

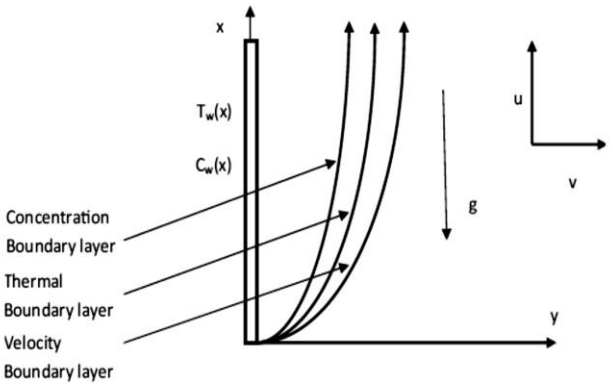

Fig. 1. Physical model and coordinate system

The continuous sheet moves in its own plane with a velocity $U_w = \frac{ax}{1-\alpha t}$ and has temperature distribution $T_w = T_\infty + \frac{bx}{(1-\propto t)^2}$ which varies with the distance *x* from the slot and time coordinate *t*.

An external variable magnetic field B_0 is applied along the positive *y*-direction. Magnetic field is sufficiently weak to ignore magnetic induction effects i.e. magnetic Reynolds number is small. The physical properties of the fluid are assumed to be uniform, isotropic, and constant. Under the usual boundary layer approximation along with Boussinesq approximation the governing equations are given by Mohanty [41]

$$\frac{\partial u}{\partial x}+\frac{\partial v}{\partial y}=0 \tag{1}$$

$$\frac{\partial u}{\partial t}+u\frac{\partial u}{\partial x}+v\frac{\partial u}{\partial y}=\left(\frac{\mu+\kappa}{\rho}\right)\frac{\partial^2 u}{\partial y^2}+\left(\frac{\kappa}{\rho}\right)\frac{\partial N}{\partial y}+g\beta\left(T-T_\infty\right)+g\beta^*\left(C-C_\infty\right)-\frac{\sigma B_0^2}{\rho}u-\frac{\upsilon}{\rho K_p^*}u \tag{2}$$

$$\frac{\partial N}{\partial t}+u\frac{\partial N}{\partial x}+v\frac{\partial N}{\partial y}=\frac{\gamma}{\rho j}\frac{\partial^2 N}{\partial y^2}-\frac{\kappa}{\rho j}\left(2N+\frac{\partial u}{\partial y}\right) \tag{3}$$

$$\frac{\partial T}{\partial t}+u\frac{\partial T}{\partial x}+v\frac{\partial T}{\partial y}=\frac{\kappa}{\rho c_p}\frac{\partial^2 T}{\partial y^2}-\frac{1}{\rho c_p}\frac{\partial q_r}{\partial y}+\left(\frac{\mu+\kappa}{\rho c_p}\right)\left(\frac{\partial u}{\partial y}\right)^2 \tag{4}$$

$$\frac{\partial C}{\partial t}+u\frac{\partial C}{\partial x}+v\frac{\partial C}{\partial y}=D_m\frac{\partial^2 C}{\partial y^2}-k_r\left(C-C_\infty\right) \tag{5}$$

The corresponding boundary conditions are

$$u=U_w(x,t),\ v=0,\ N=0,\ T=T_w(x,t)$$

$$C=C_w(x,t)\ \text{ at } y=0, u\to 0, \tag{6}$$

$$N\to 0,\ T\to T_\infty,\ C\to C_\infty \text{ as } y\to\infty$$

Thermal radiation is simulated using the Rosseland diffusion approximation and, in accordance with this, the radiative heat flux q_r is given by

$$q_r=-\frac{4\sigma^*}{3k^*}\frac{\partial T^4}{\partial y} \tag{7}$$

Where σ^* is the Stefan-Boltzman constant and K^* is the Rosseland mean absorption coefficient. It should be noted that, by using the Rosseland approximation, the present analysis is limited to optically thick fluids. If the temperature differences within the flow are sufficiently small, then equation 7 can be linearized by expanding T^4 into the Taylor series about *T*, and neglecting higher-order terms, we get

$$T^4\cong 4T_\infty^3T-3T_\infty^4 \tag{8}$$

Invoking equations 7 and 8, equation 4 can be written as

$$\frac{\partial T}{\partial t}+u\frac{\partial T}{\partial x}+v\frac{\partial T}{\partial y}=\left(\frac{\kappa}{\rho c_p}+\frac{16T_\infty^3}{3\rho c_p k^*}\right)\frac{\partial^2 T}{\partial y^2}+\left(\frac{\mu+\kappa}{\rho c_p}\right)\left(\frac{\partial u}{\partial y}\right)^2 \tag{9}$$

In order to obtain similarity solution of the problem, the following non-dimensional variables are introduced

$$\eta = \sqrt{\frac{a}{\upsilon(1-\alpha t)}}y,\ \psi = \sqrt{\frac{\upsilon a}{(1-\alpha t)}}xf(\eta),$$
$$N = \sqrt{\frac{a^3}{\upsilon(1-\alpha t)^3}}xh(\eta),$$
$$T = T_\infty + \frac{bx}{(1-\alpha t)^2}\theta(\eta) \quad (10)$$
$$C = C_\infty + \frac{cx}{(1-\alpha t)^2}\phi(\eta)$$

where η is the similarity variable and Ψ(x,y) is the stream function defined by:

$u = \frac{\partial \varphi}{\partial y} = U_w f'(\eta), v = -\frac{\partial \psi}{\partial x} = -\sqrt{\frac{\nu a}{(1-\alpha t)}} f(\eta)$

which identically satisfies equation 1. Similarity variables (10), equations 2, 3, 9 and 5 are used to obtain the following set of ordinary differential equations:

$$Nu = 1.953\left(\mathrm{Re}\,\mathrm{Pr}\frac{D}{x}\right)^{1/3} \quad \text{for} \quad \left(\mathrm{Re}\,\mathrm{Pr}\frac{D}{x}\right) \geq 33.3$$
$$Nu = 4.364 + 0.0722\,\mathrm{Re}\,\mathrm{Pr}\frac{D}{x} \quad \text{for} \quad \left(\mathrm{Re}\,\mathrm{Pr}\frac{D}{x}\right) < 33.3 \quad (11)$$

$$\lambda_o h'' + \begin{vmatrix} f & f' \\ h & h' \end{vmatrix} - \frac{A}{2}(3h + \eta h') - KB(2h + f'') = 0 \quad (12)$$

$$\left(1 + \frac{4}{3}R\right)\theta'' + \mathrm{Pr}\begin{vmatrix} f & f' \\ \theta & \theta' \end{vmatrix} - \frac{\mathrm{Pr}\,A}{2}(4\theta + \eta\theta') + \mathrm{Pr}\,Ec(1+K)f''^2 = 0 \quad (13)$$

$$\phi'' + Sc\begin{vmatrix} f & f' \\ \phi & \phi' \end{vmatrix} - \frac{ScA}{2}(4\phi + \eta\phi') - Sc\gamma\varphi = 0 \quad (14)$$

The corresponding boundary conditions are

$$f(0) = 0,\ f'(0) = 1,\ h(0) = 0,\ \theta(0) = 1,\ \phi(0) = 1 \quad (15)$$

$$f'(\infty) = 0,\ h(\infty) = 0,\ \theta(\infty) = 0,\ \phi(\infty) = 0 \quad (16)$$

where the notation primes denote differentiation with respect to η and the parameters are defined as: unsteadiness parameter, A=$\frac{\alpha}{a}$, micropolar parameter $k = \frac{k}{\mu}$, magnetic field parameter $M = \frac{\sigma B_0^2(1-\alpha t)}{\rho a}$ porous parameter $k_p = \frac{\rho k_p^* a}{\nu(1-\alpha t)}$, thermal Grashof number, $Gr = \frac{g\beta(T_w - T_\infty)x^2}{\nu U_w}$ Prandtl number Pr=$\frac{\nu}{\alpha}$, solutal Grashof number, $Gc = \frac{g\beta^*(C_w - C_\infty)X^2}{\nu U_w}$ non-dimensional material parameter $\lambda_0 = \frac{\Upsilon}{\mu j}$, non-dimensional parameter B=$\frac{\nu(1-\alpha t)}{ja}$, Eckert number Ec=$\frac{U_w^2}{c_p(T_w - T_\infty)}$, thermal radiation parameter R=$\frac{4\sigma T_\infty^3}{\kappa K^*}$, Schmidt number, Sc=$\frac{\nu}{D_m}$, chemical reaction parameter $\gamma = \frac{K_r x}{U_w}$. Also the quantities of physical interest in this problem are the local skin friction factor, couple stress factor, local rate of heat and mass transfer coefficients, which are defined by

$$C_{fx} = \frac{\tau_w\big|_{y=0}}{\rho U_w^2} = 2(1+K)\mathrm{Re}_x^{\frac{1}{2}} f''(0) \quad (17)$$

$$C_{sx} = \frac{\gamma a U_w}{\upsilon(1-\alpha t)}h'(0) \quad (18)$$

$$Nu_x = -\frac{x}{(T_w - T_\infty)}\frac{\partial T}{\partial y}\bigg|_{y=0} = -\sqrt{\mathrm{Re}_x}\,\theta'(0) \quad (19)$$

$$Sh_x = -\frac{x}{(C_w - C_\infty)}\frac{\partial C}{\partial y}\bigg|_{y=0} = -\sqrt{\mathrm{Re}_x}\,\phi'(0) \quad (20)$$

where $Re_x = \frac{U_w x}{\nu}$ is the Reynolds number.

NUMERICAL SOLUTION

The set of non-linear coupled differential equations 11 to 14 subject to the boundary conditions 15 and 16 constitute a two-point boundary value problem. In order to solve these equations numerically we follow most efficient numerical shooting technique with fourth-order Runge–Kutta scheme.

In this method it is most important to choose the appropriate finite values of $\eta \to \infty$. To select η_∞, some initial guess values are taken and solve the problem with some particular set of parameters to obtain $f''(0), h'(0), \theta'(0)$ and $\Phi'(0)$. The solution process is repeated with another large value of η_∞until two successive values of $f''(0), h'(0), \theta'(0)$ and $\Phi'(0)$ differ only after desired digit signifying the limit of the boundary along η. The last value of η_∞ is chosen as appropriate value of limit $\eta \to \infty$ for that particular set of parameters. The resulting differential equations can be integrated by fourth order Runge–Kutta

scheme. The above procedure is repeated until we get the results up to the desired degree of accuracy 10^{-6}.

RESULTS AND DISCUSSION

In order to get a clear insight of the problem, numerical computations have been carried out for various parameters such as unsteadiness parameter (A), magnetic parameter (M), porous parameter (K_P), thermal Grashof number (Gr), solutal Grashof number (Gc), Prandtl number (Pr), thermal radiation parameter (R), Eckert number (Ec), Schmidt number (Sc) and chemical reaction parameter (Υ) on velocity ($f'(\eta)$), angular velocity (h(η)), temperature (θ(η)) and concentration profiles (Φ(η)). For illustration of the results, numerical values are presented in graphical and tabular forms.

Figures 2(a-b) represent the variations of velocity and angular velocity for different values of thermal Grashof number Gr in both steady ad unsteady cases.

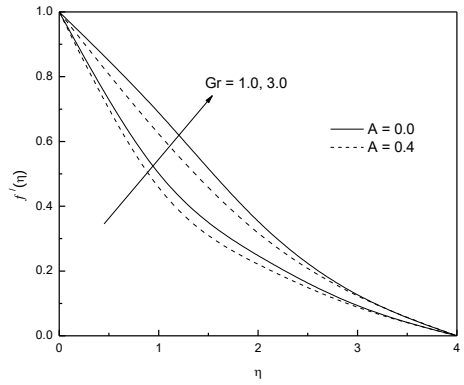

Fig. 2a. Velocity profile for various values of *Gr*

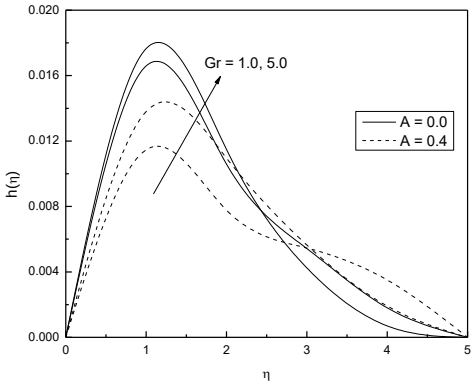

Fig. 2b. Angular velocity profile for various values of *Gr*

The Grashof number Gr is a dimensionless number in fluid dynamics and heat transfer which approximates the ratio of the buoyancy to viscous force acting on a fluid. It frequently arises in the study of situations involving natural convection. From Figure 2a, it is observed that the increasing values of Gr has made the velocity increasing in both steady and unsteady cases. From 2b, it is noticed that the angular velocity increases with Gr near the sheet ($\eta <$ 1), but it decreases after a certain distance ($1 < \eta < 5$) from the sheet for both steady A=0.0 and unsteady A=0.4 cases.

The advancement of velocity with solutal Grashof number Gc for both steady A=0.0 and unsteady A=0.4 cases is shown in Figure 3a. Figure 3b depict the influence of solutal Grashof number Gc on angular velocity h(η). As Gc increases the angular velocity also increases up to $\eta <$ 1 and then depreciates slowly with increase in η for both steady A=0.0 and unsteady A=0.4 cases.

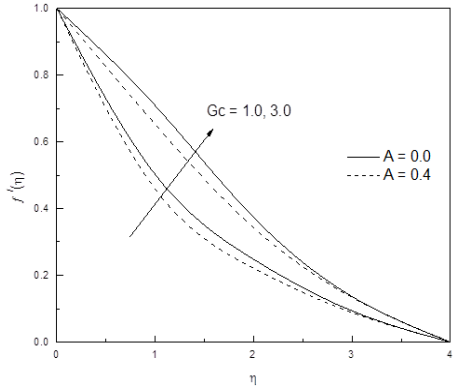

Fig. 3a. Velocity profile for various values of *Gc*

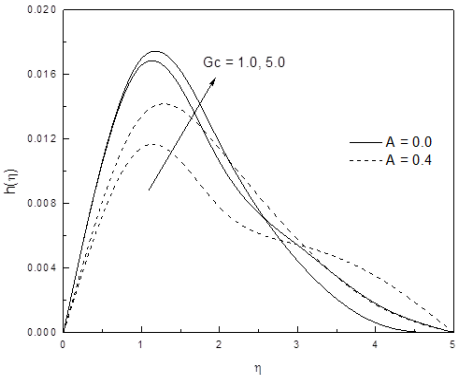

Fig. 3b. Angular velocity profile for various values of *Gc*

For both steady A=0.0 and unsteady A=0.4 cases Figures 4a to 4d provide the effect of magnetic parameter M on velocity, angular velocity, temperature and concentration profiles. It is seen from these figures that increase in magnetic parameter M decreases the velocity and increase the temperature and concentration. It is also observed that angular velocity increases rapidly up to $\eta < 1$ and then declines gradually in the flow domain $1 < \eta < 5$. As M increases, the Lorentz force, which opposes the flow, also increases and leads to enhanced deceleration of the flow. This result qualitatively agrees with the expectations, since the magnetic field exerts a retarding force on the free convection flow.

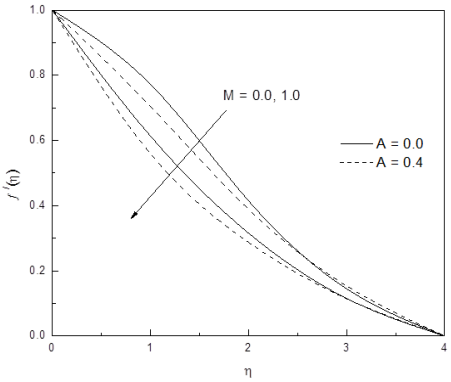

Fig. 4a. Velocity profile for various values of *M*

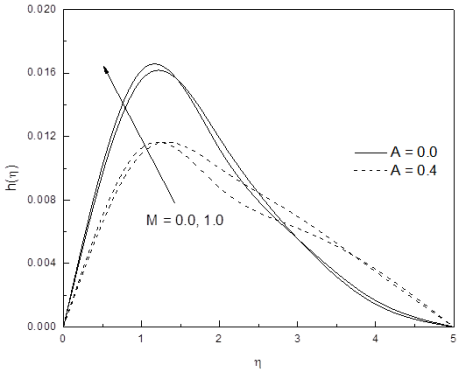

Fig. 4b. Angular velocity profile for various values of *M*

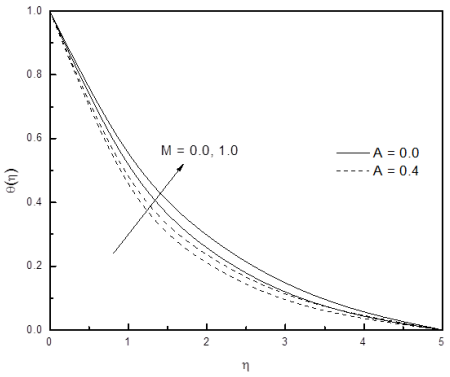

Fig. 4c. Temperature profile for various values of *M*

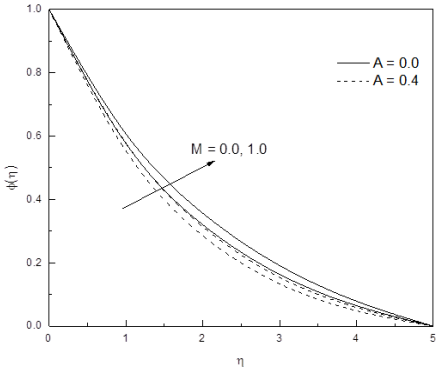

Fig. 4d. Concentration profile for various values of M

Figures 5a to 5d show the effect of porous parameter K_P on velocity, angular velocity, temperature and concentration profiles.

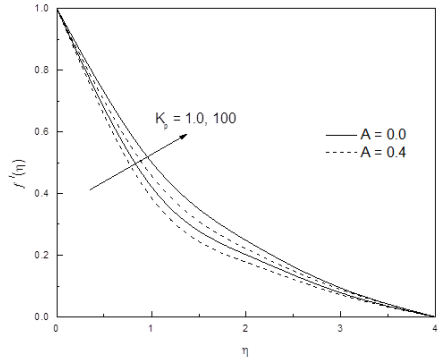

Fig. 5a. Velocity profile for various values of K_p

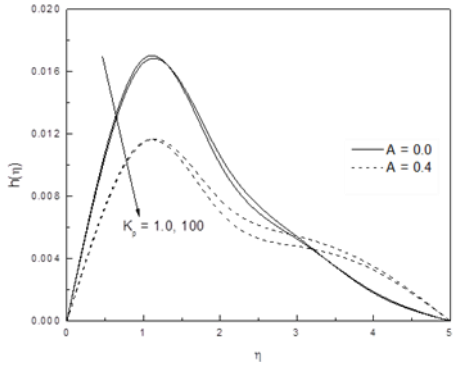

Fig. 5b. Angular velocity profile for various values of Kp

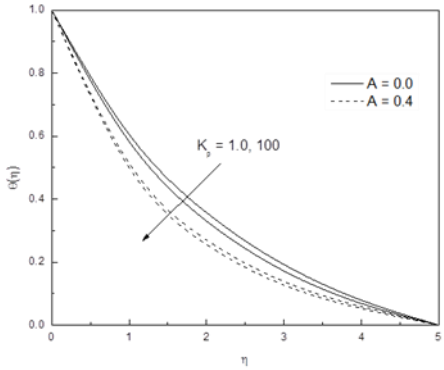

Fig. 5c. Temperature profile for various values of K_p

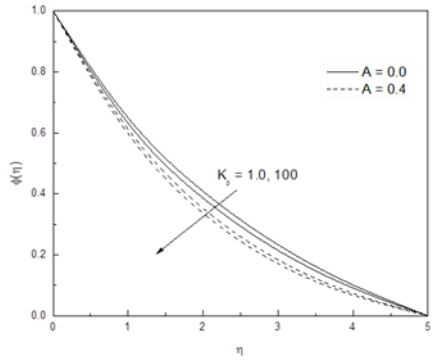

Fig. 5d. Concentration profile for various values of K_p

The one of the most important consideration of the present investigation is the saturated porous media. Porous media are widely used to insulatea heated body to maintain its temperature.

These are considered to be useful in diminishing the natural free convection which would otherwise occur inversely on the stretching surface. It is observed that velocity decreases with K_P whereas opposite phenomena is noticed in the remaining profiles for both steady A=0.0 and unsteady A=0.4 cases.

The deterioration of velocity and temperature with Prandtl number Pr for both steady A=0.0 and unsteady A=0.4 cases is shown in Figures 6a and 6b. The reason is that smaller values of *Pr* are equivalent to increasing the thermal conductivities, and therefore heat is able to diffuse away from the heated plate more rapidly than for higher values of *Pr*.

Hence in the case of smaller Prandtl numbers as the boundary layer is thicker and the rate of heat transfer is reduced.

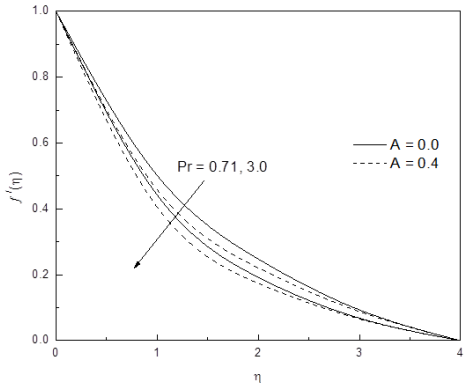

Fig. 6a. Velocity profile for various values of *Pr*

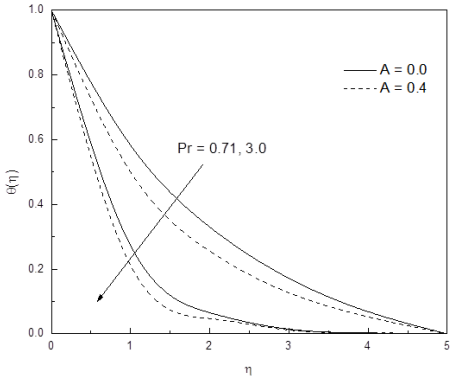

Fig. 6b. Temperature profile for various values of *Pr*

The variations of velocity, angular velocity, temperature and concentration with radiation parameter R are given in Figures 7a to 7d.

Here, we noticed that velocity and temperature enhance with R whereas concentration decreases.

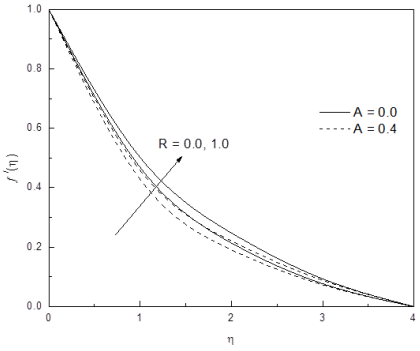

Fig. 7a. Velocity profile for various values of *R*

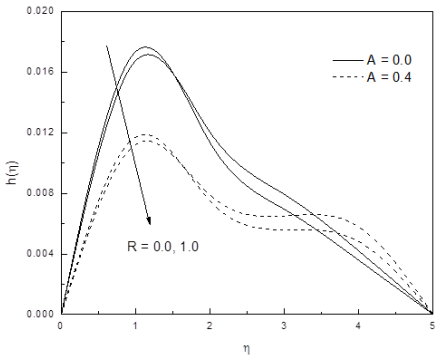

Fig. 7b. Angular velocity profile for various values of R

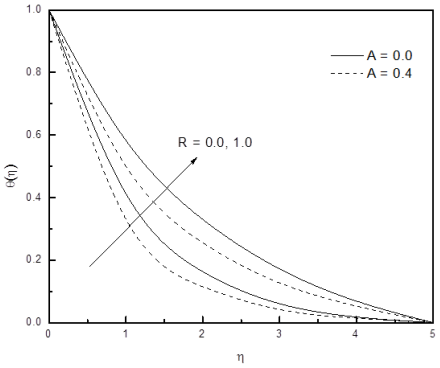

Fig. 7c. Temperature profile for various values of *R*

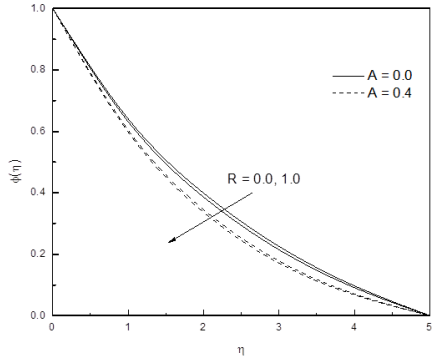

Fig. 7d. Concentration profile for various values of *R*

The effect of radiation is also to intensify the heat transfer. Thus radiation should be at its minimum in order to facilitate the cooling process.

It is also seen that angular velocity increases up to certain values of η after that it decreases with increase in η for both steady A=0.0 and unsteady A=0.4 cases.

For both steady A=0.0 and unsteady A=0.4 cases, Eckert number Ec has no significant effect on angular velocity and concentration profiles but velocity and temperature are enhancing with Ec as shown in the Figures 8a to 8d.

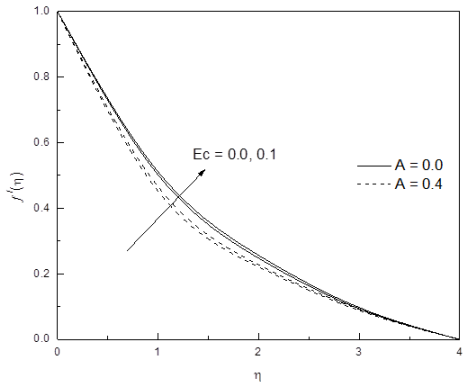

Fig. 8a. Velocity profile for various values of *Ec*

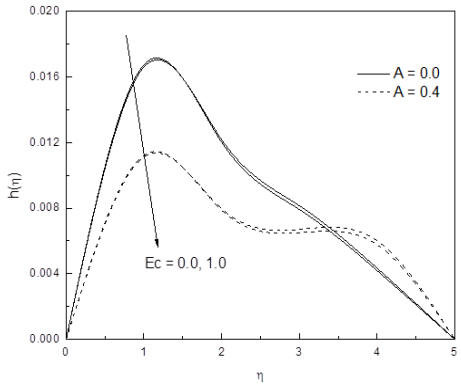

Fig. 8b. Angular velocity profile for various values of *Ec*

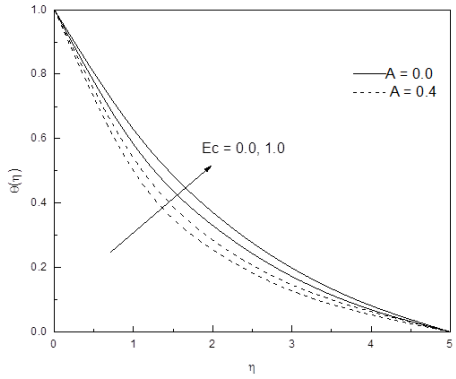

Fig. 8c. Temperature profile for various values of *Ec*

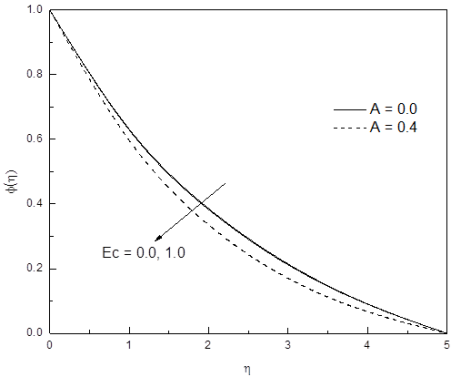

Fig. 8d. Concentration profile for various values of *Ec*

The positive Eckert number implies cooling of the plate i.e., loss of heat from the plate to the fluid. Hence, greater viscous dissipative heat causes a rise in the temperature as well as the velocity, which is evident from Figures 8a and 8b.

The influence of the Schmidt number *Sc* on the dimensionless velocity and concentration profiles are plotted in Figures 9a and 9b respectively. As the Schmidt number increases the concentration decreases. This causes the concentration buoyancy effects to decrease yielding a reduction in the fluid velocity.

The reductions in the velocity and concentration profiles are accompanied by simultaneous reductions in the velocity and concentration boundary layers. These behaviors are clear from Figures 8a and 8b.

The variation of velocity and concentration profiles with chemical reaction parameter is shown in Figures 10a and 10b for both steady and unsteady cases.It is observed that an increase in the value of chemical reaction parameter decreases the concentration of species in the boundary layer, whereas the velocity and temperature of the fluid are not significant with increase of chemical reaction parameter.

This is due to the fact that chemical reaction in this system results in consumption of the chemical and hence results in decrease of concentration profile. The most important effect is that the first order chemical reaction has a tendency to diminish the overshoot in the profiles of the solute concentration in the solutal boundary layer.

To assess the present method, comparison is made with the results of Mohanty et al. [41] as shown in Table 1(Steady case) and Table 2 (Unsteady case). The comparisons in all the above cases are found to be in excellent agreement.

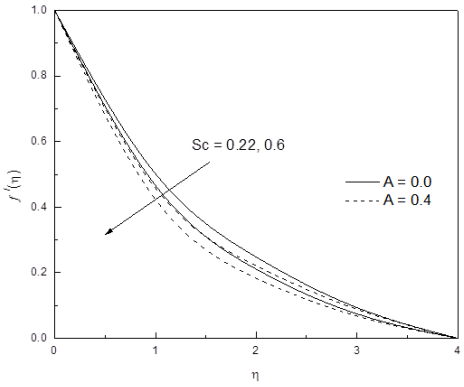

Fig. 9a. Velocity profile for various values of *Sc*

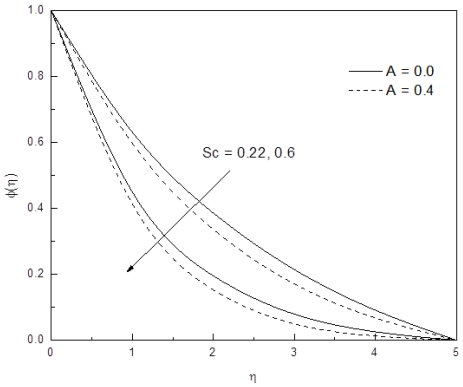

Fig. 9b. Concentration profile for various values of *Sc*

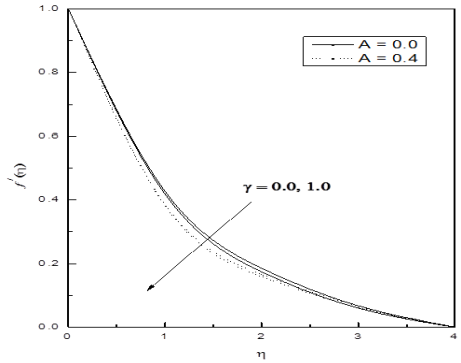

Fig. 10a. Velocity profile for various values of Υ

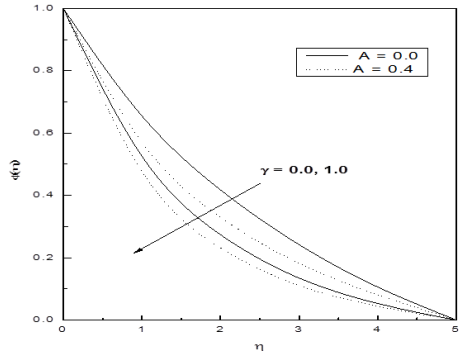

Fig. 10b. Concentration profile for various values of Υ

Table 1

Comparison of some of the values of skin-friction and couple stress coefficient obtained by the cited researcher and the present results for *A = 0.0, K = 0.5,λ_0=0.3, B = 0.1, γ = 0.0, and R = 0.0.* (Steady case).

							Mohanty et al. [41]		**Present work**	
Gr	**Gc**	**Pr**	**Sc**	**M**	**K_p**	**Ec**	**τ**	**h′(0)**	**τ**	**h′(0)**
0.0	0.0	0.72	0.00	0.0	100	0.00	-0.8186178	0.0619197	-0.818618	0.0619198
0.1	0.0	0.72	0.00	0.0	100	0.00	-0.7802563	0.0600337	-0.780257	0.0600338
0.1	0.0	0.72	0.22	0.0	100	0.00	-0.7802563	0.0600337	-0.780257	0.0600338
0.1	0.0	0.72	0.22	1.0	100	0.00	-1.1178125	0.0755773	-1.11781	0.0755776
0.1	0.0	0.72	0.22	1.0	0.5	0.00	-1.597829	0.0928029	-1.59783	0.092803
0.1	0.0	0.72	0.22	1.0	100	0.01	-1.117757	0.0755729	-1.11776	0.0755732
0.1	0.1	7.00	0.22	1.0	100	0.01	-1.0930755	0.0741295	-1.09308	0.0741297
0.1	0.1	0.72	0.22	1.0	100	0.01	-1.079285	0.07241227	-1.0724	0.0726901

Table 3 and 4 show the variations of skin friction, couple stress, heat transfer and mass transfer coefficients for different values of parameters. From Table 3, it is observed that skin friction coefficient, rate of heat and mass transfer coefficients enhance as Gr or Gc or K_P increases, but they decrease as M increases. Couple stress coefficient decreases as Gr or Gc or Kp increases, but opposite phenomena is observed with M. It is clear from Table 4 that skin friction coefficient depreciates as Pr or Ec or Sc or Υincreases, but it increases as R increases. Angular velocity rises as pr or R or Sc or Υ increases and it declines as Ec increases. Heat transfer coefficient increases and mass transfer coefficient decreases as Pr increases. Heat and mass transfer coefficients decrease as Sc increases.

It is also noticed that as R or Ec or Υ increases, heat transfer coefficient decreases and mass transfer coefficient increases.

Table 2
Comparison of some of the values of skin-friction and couple stress coefficient obtained by the cited researcher and the present results for *A = 0.4, K = 0.5, λ_0=0.3, B = 0.1, Υ=0.0 and R = 0.0.*(Unsteady case).

							Mohanty et al. [41]		Present work	
Gr	**Gc**	**Pr**	**Sc**	**M**	**K_p**	**Ec**	τ	**h′(0)**	τ	**h′(0)**
0.0	0.0	0.72	0.00	0.0	100	0.00	-0.9281049	0.0524019	-0.929107	0.0525469
0.1	0.0	0.72	0.00	0.0	100	0.00	-0.8964873	0.0511817	-0.897576	0.0513385
0.1	0.0	0.72	0.22	0.0	100	0.00	-0.8964873	0.0511817	-0.897576	0.0513385
0.1	0.0	0.72	0.22	1.0	100	0.00	-1.207273	0.0633876	-1.20737	0.0634068
0.1	0.0	0.72	0.22	1.0	0.5	0.00	-1.6639832	0.0777144	-1.6641	0.07773
0.1	0.0	0.72	0.22	1.0	100	0.01	-1.2072344	0.0633852	- 1.20695422	0.0633759
0.1	0.1	7.00	0.22	1.0	100	0.01	-1.1855281	0.0624408	-1.1854789	0.062314
0.1	0.1	0.72	0.22	1.0	100	0.01	-1.1655573	0.0614006	-1.1655462	0.061347

Table 3
Skin-friction coefficient, couple stress, rate of heat and mass transfer coefficient with *A = 0.4, K =1.0, λ_0=0.5, B = 0.3,Pr =1.0, R =0.5, Ec= 0.05, Sc=0.6, Υ=1.0.*

Gr	**Gc**	**M**	**K_p**	τ	**h′(0)**	**-θ′(0)**	**-Φ′(0)**
2.0	2.0	1.0	100	-0.657526	0.0410463	0.844124	0.718114
3.0	2.0	1.0	100	-0.358714	0.0320462	0.866132	0.736241
4.0	2.0	1.0	100	0.0273536	0.0229384	0.885447	0.742276
2.0	3.0	1.0	100	-0.341543	0.0339306	0.868656	0.758398
2.0	4.0	1.0	100	0.0607256	0.0229496	0.890072	0.766253
2.0	2.0	0.3	100	-0.319132	0.0325573	0.872192	0.771364
2.0	2.0	0.5	100	-0.483537	0.0425118	0.858833	0.770223
2.0	2.0	1.0	1.0	-0.974843	0.0536373	0.820422	0.788788
2.0	2.0	1.0	10	-0.686926	0.0441939	0.841732	0.796122

Table 4
Skin-friction coefficient, couple stress, rate of heat and mass transfer coefficient with *A = 0.4, K = 1.0, λ_0=0.3, B = 0.1,Gr = 2.0, Gc = 2.0, M = 3.0, K_p = 100.*

Pr	**R**	**Ec**	**Sc**	**Υ**	τ	**h′(0)**	**-θ′(0)**	**-Φ′(0)**
1.0	0.5	0.05	0.6	1.0	-0.277566	0.0170863	0.654174	0.338114
1.5	0.5	0.05	0.6	1.0	-0.397174	0.0183241	0.791512	0.335577
2.0	0.5	0.05	0.6	1.0	-0.471036	0.0245675	1.38339	0.32713
1.0	1.0	0.05	0.6	1.0	-0.354138	0.0255671	0.395419	0.341253
1.0	2.0	0.05	0.6	1.0	-0.240789	0.026686	0.326685	0.343084
1.0	0.5	0.1	0.6	1.0	-0.277083	0.0290563	0.450637	0.338175
1.0	0.5	0.2	0.6	1.0	-0.476481	0.0290188	0.446228	0.338251
1.0	0.5	0.05	1.0	1.0	-0.53695	0.0328487	0.545028	1.26176
1.0	0.5	0.05	2.0	1.0	-0.554765	0.0539019	0.542496	1.11877
1.0	0.5	0.05	0.6	2.0	-0.53695	0.0528487	0.645028	1.06176
1.0	0.5	0.05	0.6	3.0	-0.554765	0.0539019	0.642496	1.21877

CONCLUSIONS

Some important observations of this study can be summarized as follows:

- Buoyancy forces leads to a rise in the values of velocity.
- The effect of viscous dissipation is negligible on velocity, angular velocity and concentration profiles, but it enhances the temperature.
- The existence of magnetic field sets in Lorentz force which develops a resisting force on velocity field.
- Fluids with higher Prandtl number have low thermal conductivity.
- For steady flow, in the presence of porous parameter skin friction, heat and mass transfer coefficients decelerate whereas couple stress coefficient increases.

REFERENCES

[1] Eringen AC. Theory of micropolar fluids. Journal of Mathematics and Mechanics. 1966 Jul 1:1-8.

[2] Eringen AC. Theory of thermomicrofluids. Journal of Mathematical Analysis and Applications. 1972 May 1;38(2):480-96.

[3] Ariman TM, Turk MA, Sylvester ND. Micro continuum fluid mechanics—a review. International

Journal of Engineering Science. 1973 Aug 1;11(8):905-30.

[4] Ariman TM, Turk MA, Sylvester ND. Applications of microcontinuum fluid mechanics. International Journal of Engineering Science. 1974 Apr 1;12(4):273-93.

[5] Siddheshwar PG, Pranesh S. Effect of a non-uniform basic temperature gradient on Rayleigh–Benard convection in a micropolar fluid. International Journal of Engineering Science. 1998 Sep 30;36(11):1183-96.

[6] Siddheshwar PG, Pranesh S. Magnetoconvection in fluids with suspended particles under 1g and μg. Aerospace Science and Technology. 2002 Feb 1;6(2):105-14.

[7] Sakiadis BC. Boundary-layer behavior on continuous solid surfaces: I. Boundary-layer equations for two-dimensional and axisymmetric flow. AIChE Journal. 1961 Mar 1;7(1):26-8.

[8] Peddieson J, McNitt RP. Boundary layer theory for a micropolar fluid. Recent Advances in Engineering Science. 1970;5:405-47

[9] Chawla SS. Boundary layer growth of a micropolar fluid. International Journal of Engineering Science. 1972 Nov 1;10(11):981-7.

[10] Gorla RS, Reddy PV. Flow and heat transfer from a continuous surface in a parallel free stream of micropolar fluid. International journal of engineering science. 1987 Jan 1;25(10):1243-9.

[11] Hassanien IA, Shamardan A, Moursy NM, Subba Reddy Gorla R. Flow and heat transfer in the boundary layer of a micropolar fluid on a continuous moving surface. International Journal of Numerical Methods for Heat & Fluid Flow. 1999 Sep 1;9(6):643-59.

[12] Nazar R, Amin N, Filip D, Pop I. Stagnation point flow of a micropolar fluid towards a stretching sheet. International Journal of Non-Linear Mechanics. 2004 Sep 30;39(7):1227-35.

[13] Ishak A, Nazar R, Pop I. Heat transfer over a stretching surface with variable heat flux in micropolar fluids. Physics Letters A. 2008 Jan 28;372(5):559-61.

[14] Rahman MM, Rahman MA, Samad MA, Alam MS. Heat transfer in a micropolar fluid along a non-linear stretching sheet with a temperature-dependent viscosity and variable surface temperature. International Journal of Thermophysics. 2009 Oct 1;30(5):1649-70.

[15] Bachok N, Ishak A, Pop I. Boundary layer stagnation -point flow and heat transfer over an exponentially stretching/shrinking sheet in a nanofluid. International Journal of Heat and Mass Transfer. 2012 Dec 31;55(25):8122-8.

[16] Mohammadein AA, Gorla RS. Effects of transverse magnetic field on mixed convection in a micropolar fluid on a horizontal plate with vectored mass transfer. Acta mechanica. 1996 Mar 1;118(1):1-2.

[17] El-Hakiem MA, Mohammadein AA, El-Kabeir SM, Gorla RS. Joule heating effects on magnetohydrodynamic free convection flow of a micropolar fluid. International communications in heat and mass transfer. 1999 Feb 1;26(2):219-27.

[18] Bhargava R, Kumar L, Takhar HS. Numerical soluti - on of free convection MHD micropolar fluid flow between two parallel porous vertical plates. International journal of engineering science. 2003 Jan 31;41(2):123-36.

[19] Eldabe NT, Ouaf ME. Chebyshev finite difference method for heat and mass transfer in a hydromagnetic flow of a micropolar fluid past a stretching surface with Ohmic heating and viscous dissipation. Applied mathematics and computation. 2006 Jun 15;177(2):561-71.

[20] Hayat T, Javed T, Abbas Z. MHD flow of a micro - polar fluid near a stagnation-point towards a non-linear stretching surface. Nonlinear Analysis: Real World Applications. 2009 Jun 30;10(3):1514-26.

[21] Pal D, Chatterjee S. Heat and mass transfer in MHD non-Darcian flow of a micropolar fluid over a stretching sheet embedded in a porous media with non-uniform heat source and thermal radiation. Communications in Nonlinear Science and Numerical Simulation. 2010 Jul 31;15(7):1843-57.

[22] Aurangzaib K A , Mohammad N F, Sharidan S. Unsteady MHD mixed convection flow with heat and mass transfer over a vertical plate in a micropolar fluid-saturated porous medium. J Appl Sci Eng. 2013;16:141-50.

[23] Kelson NA, Desseaux A. Effect of surface conditions on flow of a micropolar fluid driven by a porous stretching sheet. International journal of engineering science. 2001 Nov 30;39(16):1881-97.

[24] Kelson NA , Farrell TW. Micropolar flow over a porous stretching sheet with strong suction or injection. International Communications in Heat and Mass Transfer. 2001 May 1;28(4):479-88.

[25] Bhargava R, Kumar L, Takhar HS. Finite element solution of mixed convection micropolar flow driven by a porous stretching sheet. International journal of engineering science. 2003 Nov 30;41(18):2161-78.

[26] Hayat T , Abbas Z , Javed T. Mixed convection flow of a micropolar fluid over a non-linearly stretching sheet. Physics letters A. 2008 Jan 28;372(5):637-47.

[27] Rahman MM, Sattar MA. Transient convective flow of micropolar fluid past a continuously moving vertical porous plate in the presence of radiation. Applied Mechanics and engineering.2007;12(2):497.

[28] Bhattacharyya K , Mukhopadhyay S, Layek GC , Pop I. Effects of thermal radiation on micropolar fluid flow and heat transfer over a porous shrinking sheet. International Journal of Heat and Mass Transfer. 2012 May 31;55(11):2945-52.

[29] Raptis A, Flow of a micropolar fluid past a continuously moving plate by the presence of radiation. International Journal of Heat and Mass Transfer. 1998 Sep 1;41(18):2865-6.

[30] Ali ME, Magyari E. Unsteady fluid and heat flow induced by a submerged stretching surface while its steady motion is slowed down gradually. International Journal of Heat and Mass Transfer. 2007 Jan 31;50(1):188-95.

[31] Ishak A , Nazar R, Pop I. Heat transfer over a stretching surface with variable heat flux in micropolar fluids. Physics Letters A. 2008 Jan 28;372(5):559-61.

[32] Ibrahim SM, Reddy TS, Reddy NB. Radiation and mass transfer effects on MHD free convection flow of a micropolar fluid past a stretching surface embedded in a non-Darcian porous medium with heat generation. ISRN Thermodynamics. 2013 Feb 21;2013.

[33] Mabood F, Ibrahim S.M, Rashidi M.M, Shadloo M.S, Lorenzin Gi. Non-uniform heat source/sink and Soret effects on MHD non-Darcian convective flow past a stretching sheet in a micropolar fluid with radiation, International Journal of heat and Mass Transfer.2016 Feb 29;93: 674 –82.

[34] Hayat T, Qasim M. Effects of thermal radiation on unsteady magnetohydrodynamic flow of a micropolar fluid with heat and mass transfer. Zeitschrift für Naturforschung A. 2010 Nov 1;65(11):950-60.

[35] El-Aziz MA. Mixed convection flow of a micropolar fluid from an unsteady stretching surface with viscous dissipation. Journal of the Egyptian Mathematical Society. 2013 Oct 31;21(3):385-94.

[36] Hsiao KI. Heat and mass transfer for micropolar flow with radiation effect past a nonlinearly stretching sheet, Heat and Mass Transfer, 46, 413-419, 2010.steady motion is slowed down gradually. International Journal of Heat and Mass Transfer. 2007 Jan 31;50(1):188-95.

[37] Cortell R. MHD flow and mass transfer of an electrically conducting fluid of second grade in a porous medium over a stretching sheet with chemically reactive species. Chemical Engineering and Processing: Process Intensification. 2007 Aug 31;46(8):721-8.

[38] Mohamed RA, Abo-Dahab SM. Influence of chemical reaction and thermal radiation on the heat and mass transfer in MHD micropolar flow over a vertical moving porous plate in a porous medium with heat generation. International Journal of Thermal Sciences. 2009 Sep 30;48(9):1800-13.

[39] Pal D, Biswas S. Perturbation analysis of magnet ohydrodynamics oscillatory flow on convective-radiative heat and mass transfer of micropolar fluid in a porous medium with chemical reaction. Engineering Science and Technology, an International Journal. 2016 Mar 31;19(1):444-62.

[40] Mabood F, Ibrahim SM. Effects of Soret and Non-Uniform Heat Source on MHD Non-Darcian Convective Flow over a Stretching Sheet in a Dissipative Micropolar Fluid with Radiation. Journal of Applied Fluid Mechanics. 2016 Nov 1;9(5).

[41] Mohanty B, Mishra SR, Pattanayak HB. Numerical investigation on heat and mass transfer effect of micropolar fluid over a stretching sheet through porous media. Alexandria Engineering Journal. 2015 Jun 30;54(2):223-32.